

Supplementary Online Information

Evolution of acyl-ACP-thioesterases and ketoacyl-synthases revealed by protein-protein interactions

Joris Beld, Jillian L. Blatti, Craig Behnke, Michael Mendez and Michael D. Burkart

Department of Chemistry and Biochemistry, University of California-San Diego, La Jolla, CA 92093-0358, USA

Table of Contents

Table S1 – Overview protein homology modeling	2
Table S2 – Literature extracted GCMS data for TE subfamilies	3
Figure S1 – Sequence alignment of ACP, KSII and TE	5
Figure S2 – Phylogeny of acyl carrier protein (ACP).....	6
Figure S3 – Phylogeny of ketoacyl synthases (KSI/KSII/KSIII).....	8
Figure S4 - Phylogeny of acyl-ACP thioesterases.....	9
Figure S5– Phylogeny of malonyl-CoA acyltransferase (MCAT, fabD).....	11
Figure S6– Phylogeny of malonyl-CoA acyltransferase (MCAT, fabD).....	12
Figure S7– Phylogeny of acyl-ACP ketoreductase (KR, FabG).....	13
Figure S8– Phylogeny of acyl-ACP ketoreductase (KR, FabG).....	14
Figure S9– Phylogeny of acyl-ACP dehydratase (DH, FabZ)	15
Figure S10– Phylogeny of acyl-ACP dehydratase (DH, FabZ)	16
Figure S11– Phylogeny of acyl-ACP dehydratase (DH, FabA).....	17
Figure S12– Phylogeny of enoyl ACP reductase (ER, FabI).....	18
Figure S13– Phylogeny of enoyl ACP reductase (ER, FabI).....	19
Figure S14 – Docking of EcACP with various KSs.....	20
Figure S15 – Docking of extracted EcACP with EcKSII and CrTE	21
Figure S16 – Docking of Cr-cACP with various KSs	22
Figure S17 – Docking of RcACP with various KSs.....	23
Figure S18 – Docking of ACPs with CrTE	24
Figure S19 – ACP complementation	25
Figure S20 – GCMS profiles of sequenced green microalgae	26
References.....	27

Table S1 – Overview protein homology modeling

Name	Protein	Q-state	Uniprot entry	From	Models after PDB	RMSD** (Å)	Identity ****	Qmean 4*****
RcKS2	FabF	Dimer	Q41134	<i>E. coli</i>	3ho9*	0.079- A	45%	0.59
RcACP	ACP	Mono	B9RR02	<i>T. thermophiles HB8</i>	1x3o	0.083- A	44%	0.8
VhKS2	FabF	Dimer	P55338	<i>E. coli</i>	3ho9	0.078- A	75%	0.63
VhACP	ACP	Mono	P0A2W3	<i>V. harveyi</i>	2l0q	0- A	97%	0.86
CrKS2	KSII	Dimer	A8JCK1	<i>T. thermophiles HB8</i>	1j3n	0.227- A	47%	0.52
Cr-cACP**	ACP	Mono	Q6UKY5	<i>A. aeolicus</i>	2eht	0.08- A	53%	0.7
Cr-mACP**	ACP	Mono	Q6UKY4	<i>B. subtilis</i>	2x2b	0.09- A	52%	0.3
CrTE	TE	Mono	A8HY17	<i>L. plantarum</i>	2own	0.47- A	18%	0.4
EcACP	ACP	Mono	P0A6A8	<i>E. coli</i>	1t8k	-	Xray	-
EcACP***	ACP	Mono	P0A6A8	<i>E. coli</i>	3ejb	-	Xray	-
EcKS2	KS2	Dimer	P0AAI5	<i>E. coli</i>	2gfw	-	Xray	-

*With itasser after 1e5m

**RMSD values obtained by 'align' algorithm in Pymol

***Extracted from the co-crystal structure of EcACP with P450biol from *B. subtilis*

**** Sequence identity between protein and 'modeled after' protein

***** Qmean4 is a reliability score of the generated homology model. The closer to 1 the better the model. (Benkert et al. 2008)

Table S2 – Literature extracted GCMS data for TE subfamilies

	A	A	A	B	D	D	E	F	F	F	G	G	G	I	I	J
	<i>Cuphea strigulosa</i>	<i>Cuphea carthagenensis</i>	<i>Cuphea wrightii</i>	<i>Physcomitrella patens</i>	CS-98- <i>Micromonas nuscilla</i>	CS-170- <i>Micromonas nuscilla</i>	<i>Desulfovibrio vulgaris</i>	<i>Bacteroides fragilis</i>	<i>Bacteroides theta</i>	<i>Bacteroides fragilis</i>	Hobbs3- <i>Clostridium nerfrinnens</i>	KA137- <i>Clostridium nerfrinnens</i>	E98- <i>Clostridium perfringens</i>	<i>Geobacillus stearothermophilus</i>	<i>Geobacillus thermoglucosidius</i>	<i>Lactobacillus helveticus</i>
C6:0	0.5	1.1	0.0	0.0	0.0	0.0	0.0	0.0	0.0	0.0	0.0	0.0	0.0	0.0	0.0	0.0
C8:0	0.7	2.0	0.1	0.0	0.0	0.0	0.0	0.0	0.0	0.0	0.0	0.0	0.0	0.0	0.0	0.0
C10:0	4.2	9.9	29.5	0.0	0.0	0.0	0.0	0.0	0.0	0.0	0.0	0.0	3.0	0.0	0.0	0.6
C12:0	53.0	58.5	54.6	0.0	0.0	0.0	0.0	0.0	0.0	0.0	25.5	36.0	33.0	0.0	0.0	1.8
C12:2	0.0	0.0	0.0	0.8	0.0	0.0	0.0	0.0	0.0	0.0	0.0	0.0	0.0	0.0	0.0	0.0
C14:0	22.4	12.0	5.2	0.0	15.9	15.1	0.3	0.0	1.1	0.2	25.5	22.1	20.0	0.8	1.1	12.4
iC14:0	0.0	0.0	0.0	0.0	0.0	0.0	0.0	0.0	0.8	0.0	0.0	0.0	0.0	0.2	0.3	0.0
C14:1	5.0	3.5	0.0	0.0	0.0	0.0	0.0	0.0	0.0	0.0	3.2	1.2	4.0	0.0	0.0	0.0
aiC15:0	0.0	0.0	0.0	0.0	0.0	0.0	2.2	35.3	32.2	32.9	0.0	0.0	0.0	3.7	2.4	0.0
iC15:0	0.0	0.0	0.0	0.0	0.0	0.0	12.5	17.1	9.1	14.7	3.2	2.3	3.0	17.9	17.0	0.0
C15:0	0.0	0.0	0.0	0.7	0.0	0.7	0.6	7.9	7.9	0.0	4.3	2.3	2.0	3.1	2.9	0.0
iC15:1	0.0	0.0	0.0	0.0	0.0	0.0	0.4	0.0	0.0	0.0	0.0	0.0	0.0	0.0	0.0	0.0
iC16:0	0.0	0.0	0.0	0.0	0.0	0.0	0.8	0.0	0.0	0.0	0.0	0.0	0.0	0.0	0.0	0.0
C16:0	3.8	3.0	2.3	36.2	49.1	46.4	22.1	3.9	4.0	5.8	8.5	9.3	8.0	13.9	18.5	35.0
10Me C16:0	0.0	0.0	0.0	0.0	0.0	0.0	0.0	0.0	0.0	0.0	2.1	0.0	4.0	7.8	15.2	0.0
C16:1	0.0	0.0	0.0	1.9	10.5	7.0	11.7	0.0	0.0	0.0	5.3	1.2	1.0	0.0	0.0	2.5
C16:2	0.0	0.0	0.0	1.3	0.0	0.0	0.0	0.0	0.0	0.0	0.0	0.0	0.0	0.0	0.0	0.0
C16:3	0.0	0.0	0.0	4.3	0.0	0.0	0.0	0.0	0.0	0.0	0.0	0.0	0.0	0.0	0.0	0.0
C17:0	0.0	0.0	0.0	0.0	0.0	0.0	1.9	0.0	1.7	0.0	4.3	5.8	5.0	5.5	2.5	0.0
iC17:0	0.0	0.0	0.0	0.0	0.0	0.0	8.1	0.0	0.0	0.0	0.0	0.0	0.0	25.4	30.0	0.0
aiC17:0	0.0	0.0	0.0	0.0	0.0	0.0	2.3	0.0	0.0	0.0	0.0	0.0	0.0	18.9	6.4	0.0
aiC17:1	0.0	0.0	0.0	0.0	0.0	0.0	1.8	0.0	0.0	0.0	0.0	0.0	0.0	0.0	0.0	0.0
C17:1	0.0	0.0	0.0	0.0	0.0	0.0	0.5	0.0	0.0	0.0	0.0	0.0	0.0	0.0	0.0	0.0
iC17:1	0.0	0.0	0.0	0.0	0.0	0.0	27.9	0.0	0.0	0.0	0.0	0.0	0.0	0.0	0.0	0.0
iC18:0	0.0	0.0	0.0	0.0	0.0	0.0	0.0	0.0	0.0	0.0	0.0	0.0	0.0	0.5	1.3	0.0
C18:0	1.0	0.8	0.0	0.0	3.6	4.1	3.1	0.0	0.0	0.0	8.5	8.1	7.0	1.5	1.4	12.0
C18:1	4.6	4.6	3.1	3.1	20.9	26.6	2.8	0.0	0.0	0.0	4.3	2.3	2.0	0.0	0.0	24.0
C18:2	4.8	4.7	5.2	15.0	0.0	0.0	0.0	0.0	0.0	0.0	0.0	0.0	0.0	0.0	0.0	6.7
C18:3	0.0	0.0	0.0	13.0	0.0	0.0	0.0	0.0	0.0	0.0	0.0	0.0	0.0	0.0	0.0	0.0
C18:4	0.0	0.0	0.0	0.7	0.0	0.0	0.0	0.0	0.0	0.0	0.0	0.0	0.0	0.0	0.0	0.0
iC19:0	0.0	0.0	0.0	0.0	0.0	0.0	0.0	0.0	0.0	0.0	0.0	0.0	0.0	0.4	0.3	0.0
aiC19:0	0.0	0.0	0.0	0.0	0.0	0.0	0.0	0.0	0.0	0.0	0.0	0.0	0.0	0.4	0.6	0.0
C19:0	0.0	0.0	0.0	0.0	0.0	0.0	0.0	0.0	0.0	0.0	0.0	0.0	0.0	0.0	0.1	0.0

cyC19:0	0.0	0.0	0.0	0.0	0.0	0.0	0.0	0.0	0.0	0.0	0.0	0.0	0.0	0.0	0.0	4.3
C19:1	0.0	0.0	0.0	0.0	0.0	0.0	0.1	0.0	0.0	0.0	0.0	0.0	0.0	0.0	0.0	0.0
C20:0	0.0	0.0	0.0	0.0	0.0	0.0	0.0	0.0	0.0	0.0	5.3	9.3	8.0	0.0	0.0	0.0
C20:1	0.0	0.0	0.0	0.0	0.0	0.2	0.0	0.0	0.0	0.0	0.0	0.0	0.0	0.0	0.0	0.6
C20:3	0.0	0.0	0.0	3.3	0.0	0.0	0.0	0.0	0.0	0.0	0.0	0.0	0.0	0.0	0.0	0.0
C20:4	0.0	0.0	0.0	17.6	0.0	0.0	0.0	0.0	0.0	0.0	0.0	0.0	0.0	0.0	0.0	0.0
C20:5	0.0	0.0	0.0	1.7	0.0	0.0	0.0	0.0	0.0	0.0	0.0	0.0	0.0	0.0	0.0	0.0
C22:0	0.0	0.0	0.0	0.0	0.0	0.0	0.2	0.0	0.0	0.0	0.0	0.0	0.0	0.0	0.0	0.0
C22:3	0.0	0.0	0.0	0.7	0.0	0.0	0.0	0.0	0.0	0.0	0.0	0.0	0.0	0.0	0.0	0.0
n15h	0.0	0.0	0.0	0.0	0.0	0.0	0.0	0.8	2.3	0.0	0.0	0.0	0.0	0.0	0.0	0.0
i16h	0.0	0.0	0.0	0.0	0.0	0.0	0.0	0.0	1.0	0.0	0.0	0.0	0.0	0.0	0.0	0.0
n16h	0.0	0.0	0.0	0.0	0.0	0.0	0.0	5.7	6.3	8.2	0.0	0.0	0.0	0.0	0.0	0.0
i17h	0.0	0.0	0.0	0.0	0.0	0.0	0.0	25.8	26.3	38.2	0.0	0.0	0.0	0.0	0.0	0.0
a17h	0.0	0.0	0.0	0.0	0.0	0.0	0.0	2.3	5.2	0.0	0.0	0.0	0.0	0.0	0.0	0.0
n17h	0.0	0.0	0.0	0.0	0.0	0.0	0.0	1.3	2.0	0.0	0.0	0.0	0.0	0.0	0.0	0.0

Table S2 – Literature extracted GCMS data for TE subfamilies Extracted GCMS profiles of various species, which matches the TEs Jing et al. (Jing et al. 2011) expressed in *E. coli* strain K27. Normalized data was taken from various sources: *Cuphea strigulosa* (Ghebretinsae et al. 2008), *Cuphea carthagenensis* (Ghebretinsae et al. 2008), *Cuphea wrightii* (Ghebretinsae et al. 2008), *Physcomitrella patens* (Grimsley et al. 1981), *CS-98 Micromonas pusilla* (Dunstan et al. 1992), *CS-170 Micromonas pusilla* (Dunstan et al. 1992), *Desulfovibrio vulgaris* (Edlund et al. 1985), *Bacteroides fragilis* (Brondz et al. 1991), *Bacteroides theta* (Mayberry 1980), *Bacteroides fragilis* (Mayberry 1980), *Clostridium perfringens* (Moss and Lewis 1967), *Geobacillus stearothermophilus* (Siristova et al. 2009), *Geobacillus thermoglucosidasius* (Siristova et al. 2009), and *Lactobacillus helveticus* (Guerzoni et al. 2001). Fatty acid nomenclature: a or ai = anti-iso branched, i = iso branched, cy = containing a cyclopropane, h = hydroxylated; the number itself corresponds to the number of carbons and the number after the : corresponds to the number of unsaturations. The green shading corresponds to the percentage (normalized to 100%) of the fatty acid present.

Figure S1 – Sequence alignment of ACP, KSII and TE

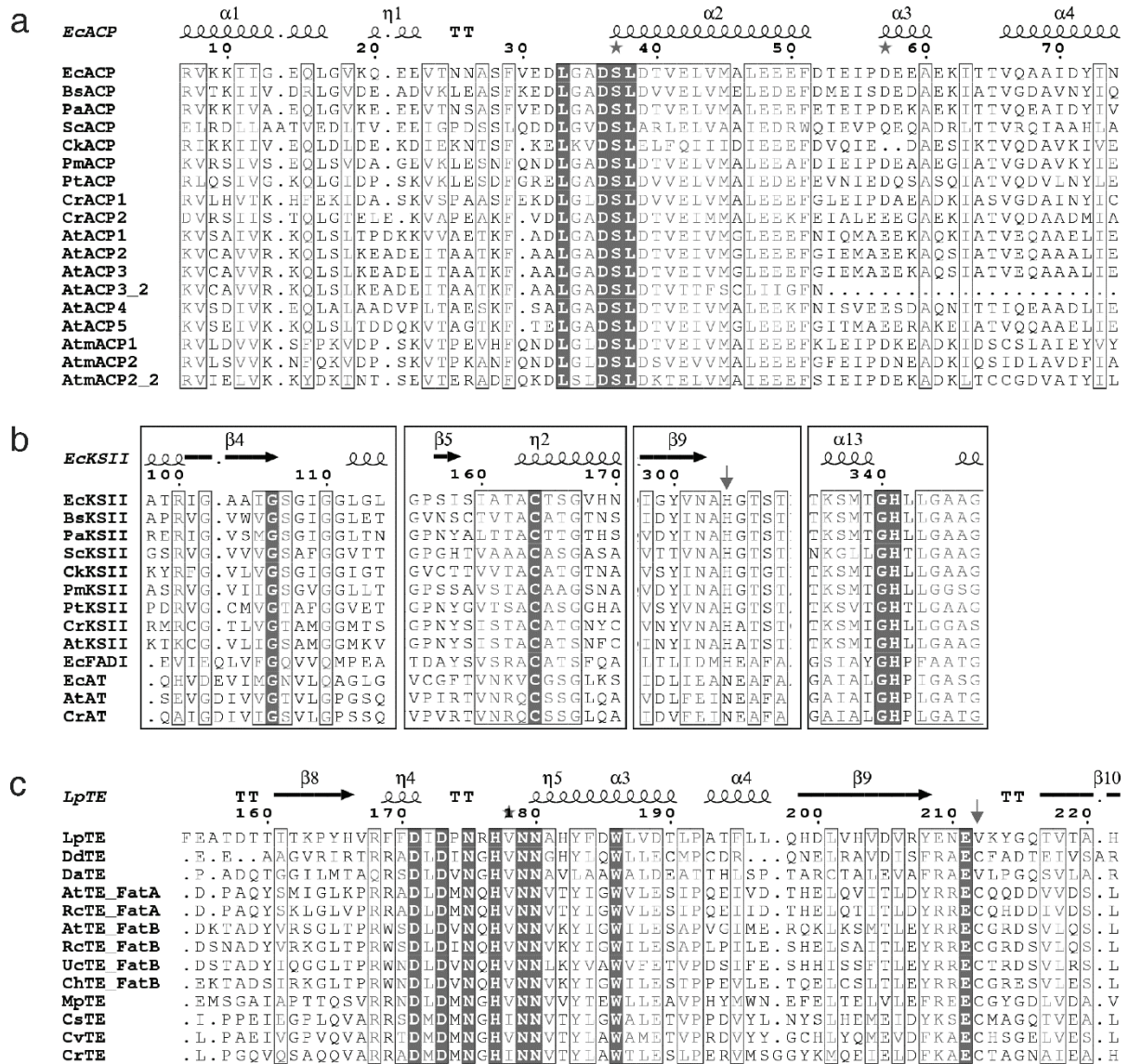
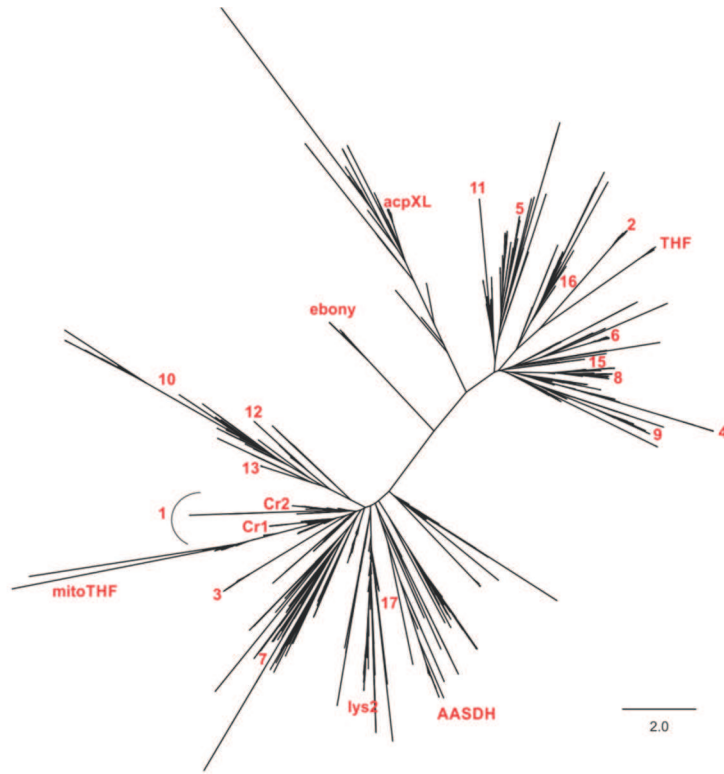


Figure S1. Sequence alignments of FAS enzymes. Structure-based alignments of bacterial, algal, and plant FAS enzymes were produced using Toffee (Notredame et al. 2000), MUSCLE (Edgar 2004) and ESPrift (Gouet et al. 1999). a) acyl carrier protein (ACP); the serine residue carrying the 4'-phosphopantetheine arm is labeled with a star. b) ketoacyl synthase II (FabF) and thiolases (AT); the active site Cys164, His304, His/Asn341 (marked with an arrow) is highly conserved. c) acyl-ACP thioesterase (TE); the active site His177, Asn179 and Cys212 (marked with an arrow) is highly conserved. Complete sequence alignments are shown in Figure S1-S5. Ec = *Escherichia coli*, Bs = *Bacillus subtilis*, Pa = *Pseudomonas aeruginosa*, Sc = *Streptomyces coelicolor*, Ck = *Clostridium kluyveri*, Pm = *Prochlorococcus marinus*, Pt = *Phaeodactylum tricoratum*, Cr = *Chlamydomonas reinhardtii*, Dd = *Desulfovibrio desulfuricans*, Da = *Desulfovibrio africanus*, Rc = *Ricinus communis*, Uc = *Umbellularia californica*, Ch = *Cuphea hookeriana*, Mp = *Micromonas pusilla*, Cs = *Coccomyxa subellipsoidea* C-169, Cv = *Chlorella variabilis* and Cr = *Chlamydomonas reinhardtii*.

Figure S2 – Phylogeny of acyl carrier protein (ACP)

A



B

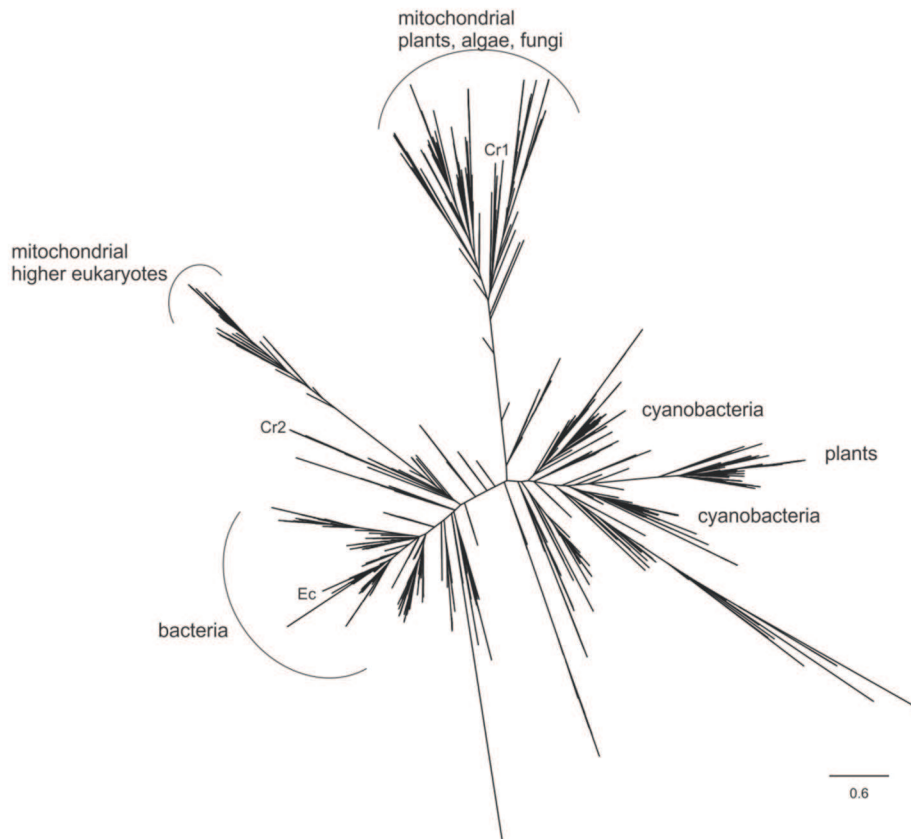


Figure S2 – Phylogeny of acyl carrier protein (ACP). Detailed phylogenetic analysis of the acyl carrier proteins was conducted with sequences obtained from the UniprotKB database and the NCBI database. A) Hundred unique sequences from each of the 16 families identified by Cantu et al. (Cantu et al. 2012) were collected by psi-blasting the archetypical ACP against the NCBI database. We added NodF, ACPXL, Rkpf, Smb20651, ACPM, fTHF-DH, AASDH, Lys2, Ebony, CAR, CrACP1 and CrACP2,(Byers and Gong 2007) resulting in ~3000 unique sequences. Sequences were aligned with MUSCLE and FasttreeMP was used to construct a phylogenetic tree. The numbers in red correspond to the families identified by Cantu et al. (Cantu et al. 2012) B) We constructed a separate tree of family 1, which contains both type II and mitochondrial fatty acid synthase ACPs. Here, we psi-blasted *E. coli* ACPP, CrACP1 and CrACP2, and collected ~2000 sequences, which were aligned with MUSCLE and a phylogenetic tree constructed using FasttreeMP.

Figure S3 – Phylogeny of ketoacyl synthases (KSI/KSII/KSIII)



Figure S3 – Phylogeny of ketoacyl synthases Detailed phylogenetic analysis of the thiolase superfamily was conducted with sequences obtained from the UniprotKB database. Sequences were aligned with MUSCLE and NJ tree constructed using MEGA.

Figure S4 - Phylogeny of acyl-ACP thioesterases

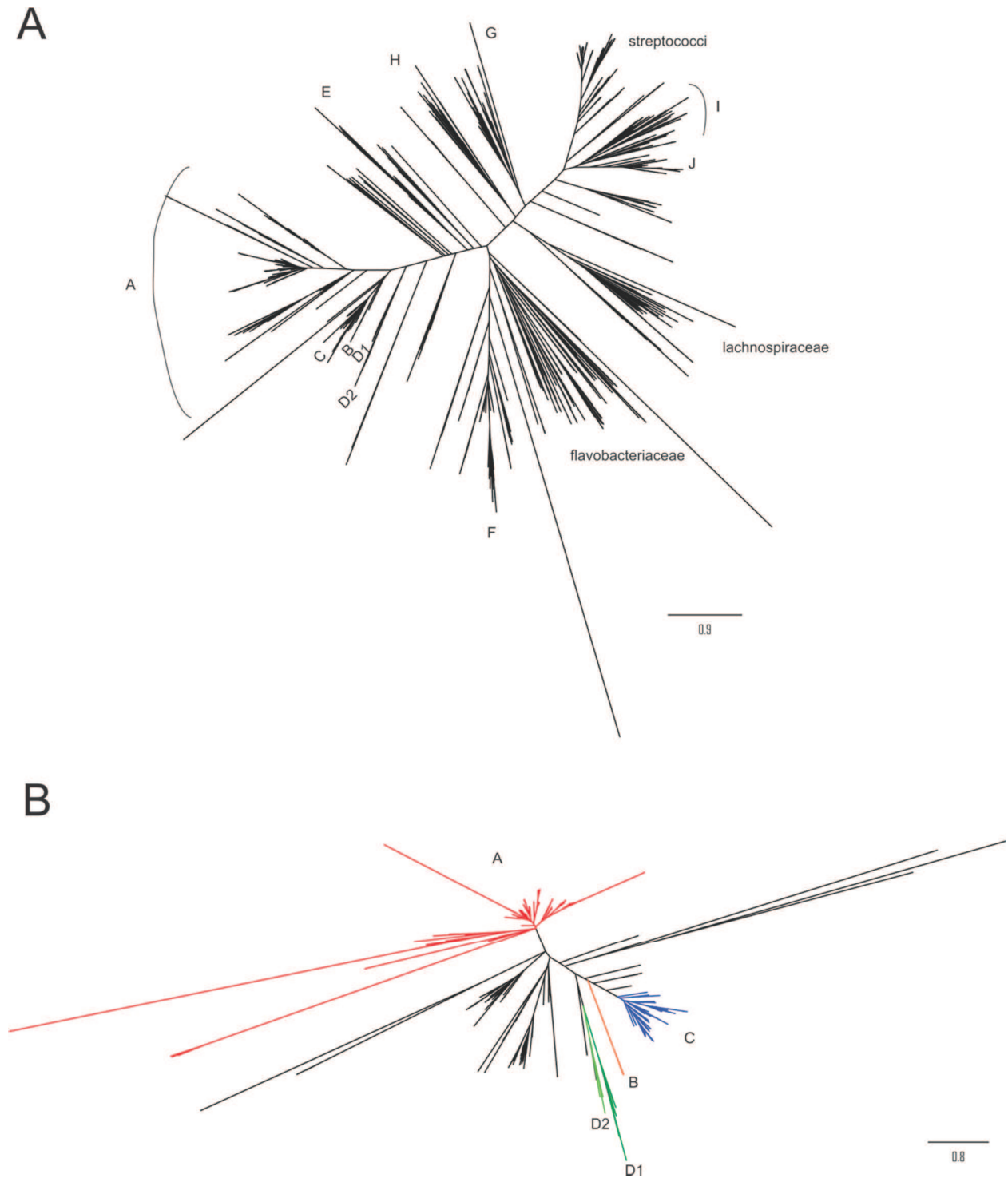


Figure S4 – Phylogeny of acyl-ACP thioesterases A) Detailed phylogenetic analysis of the acyl-ACP thioesterase family [TE14](#) (Cantu et al. 2010) was conducted with sequences obtained by Psi-Blasting FatA, FatB and Fat1 from various organisms against the NCBI database. From unique sequences, a large (>500 TEs)

phylogenetic tree was constructed using MUSCLE and Fasttree. The letters A-J correspond to the **sub**families identified by Jing et al.(Jing et al. 2011), see also table below. **B**) using only sequences of plant and algae! acyl-ACP thioesterases a smaller tree shows the separation between families A, B, C, D1 and D2.

Family	Representatives
A	Planta (FatA)
B	Mosses (<i>Physcomitrella</i>)
C	Planta (FatB)
D1	Green algae (<i>Micromonas</i> , <i>Ostreococcus</i>)
D2	Green algae (<i>Chlamydomonas</i> , <i>Volvox</i>)
E	<i>Desulfovibrio vulgaris</i>
G	<i>Clostridium perfringens</i>
H	<i>Clostridium asparagiforme</i>
I	<i>Geobacillus sp.</i>
J	<i>Lactobacillus brevis</i>

Figure S5– Phylogeny of malonyl-CoA acyltransferase (MCAT, fabD)

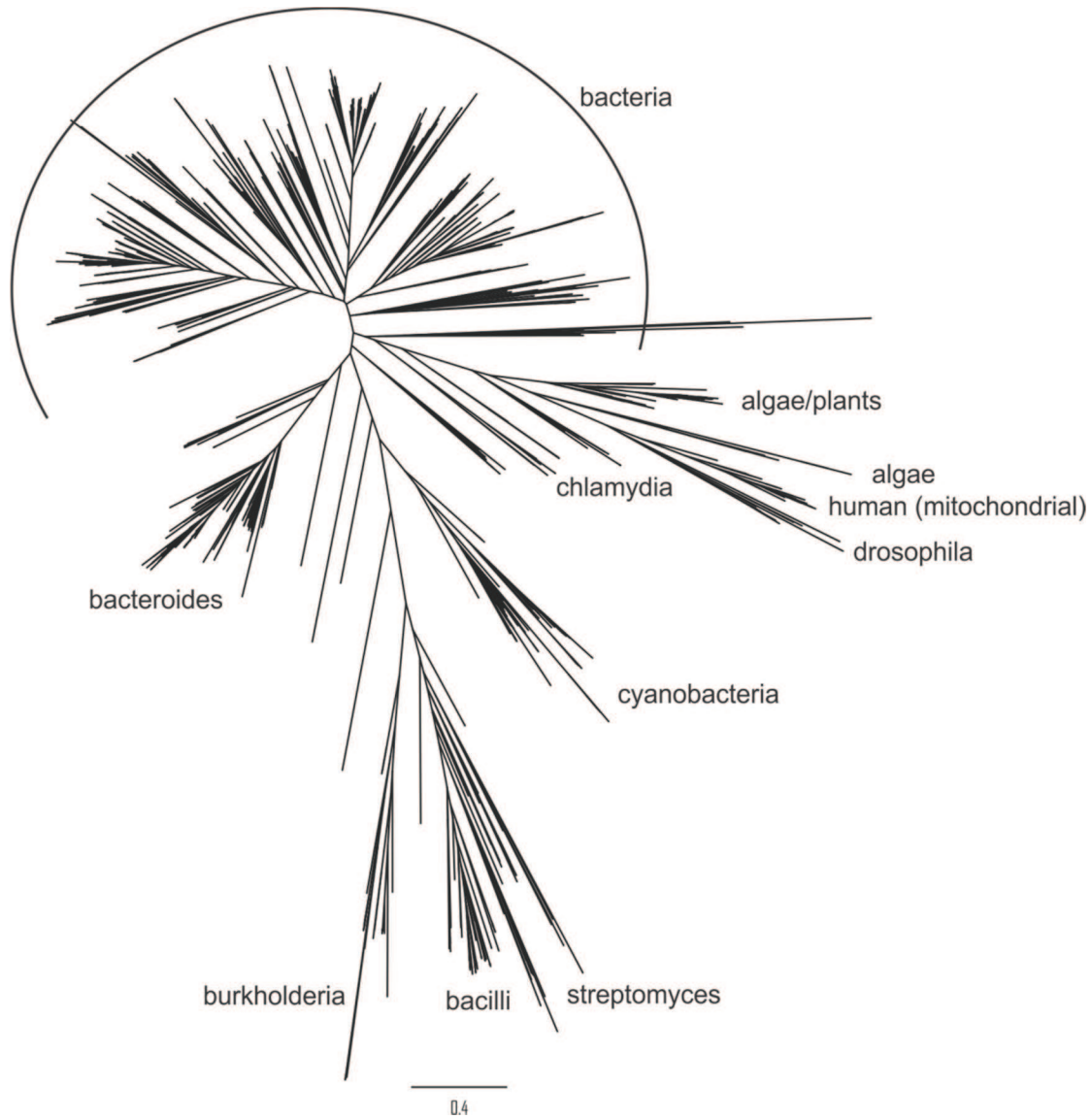


Figure S5 – Phylogeny of malonyl Coa acyltransferases (MCAT, FabD). Sequences were taken together from psi-blasting alga *C. reinhardtii*'s MCAT and psi-blasting cyanobacteria *A. variabilis* MCAT against the entire NCBI genome database and 2000 sequences were analyzed for duplicates (~50%), taxon names shortened using Mesquite, aligned using MUSCLE, a phylogenetic tree built with FastTree and visualized using Figtree.

Figure S6– Phylogeny of malonyl-CoA acyltransferase (MCAT, fabD)

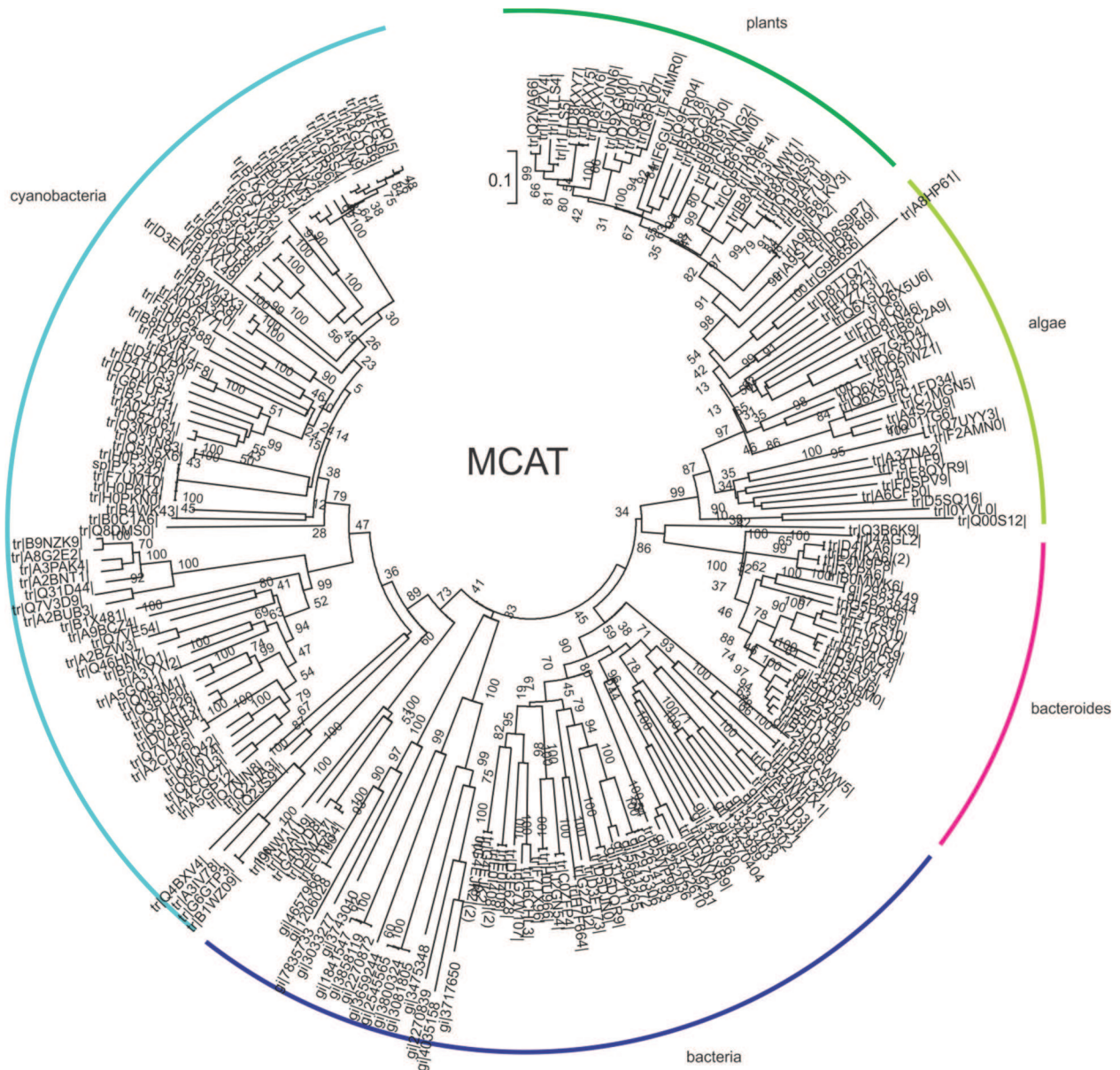


Figure S6 – Phylogeny of malonyl-CoA acyltransferases (MCAT, FabD). Neighbour Joining phylogenetic tree, constructed using MEGA 5.2, from 200 plant, algal, cyanobacterial and bacterial MCAT sequences.

Figure S7– Phylogeny of acyl-ACP ketoreductase (KR, FabG)

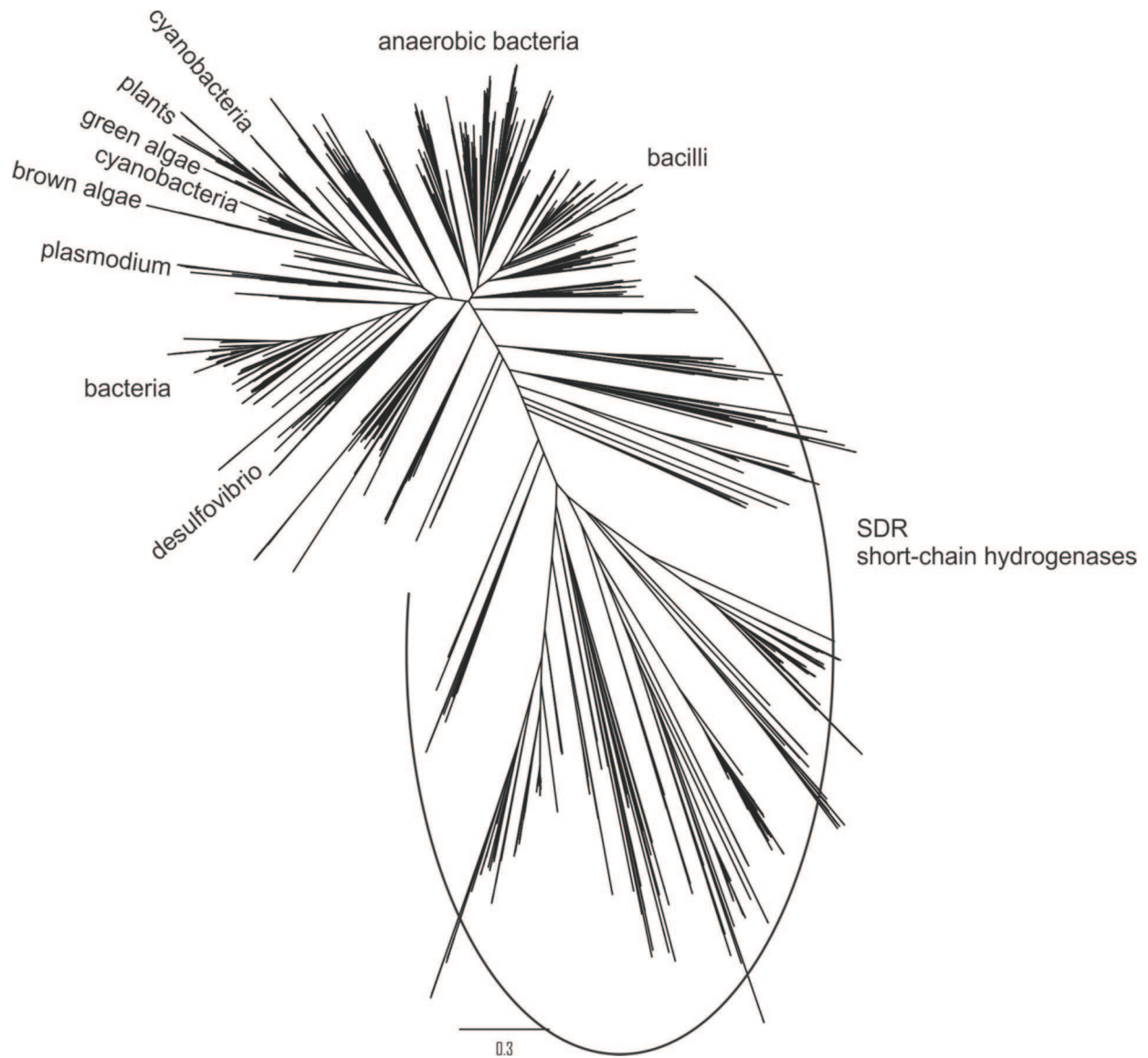


Figure S7 – Phylogeny of ketoacyl ACP reductases (KR, FabG) Sequences were taken together from psi-blasting *C. reinhardtii*'s KR and psi-blasting *A. variabilis* KR against the entire NCBI genome database and 2000 sequences were analyzed for duplicates (~50%), taxon names shortened using Mesquite, aligned using MUSCLE, a phylogenetic tree built with FastTree and visualized using Figtree.

Figure S8– Phylogeny of acyl-ACP ketoreductase (KR, FabG)

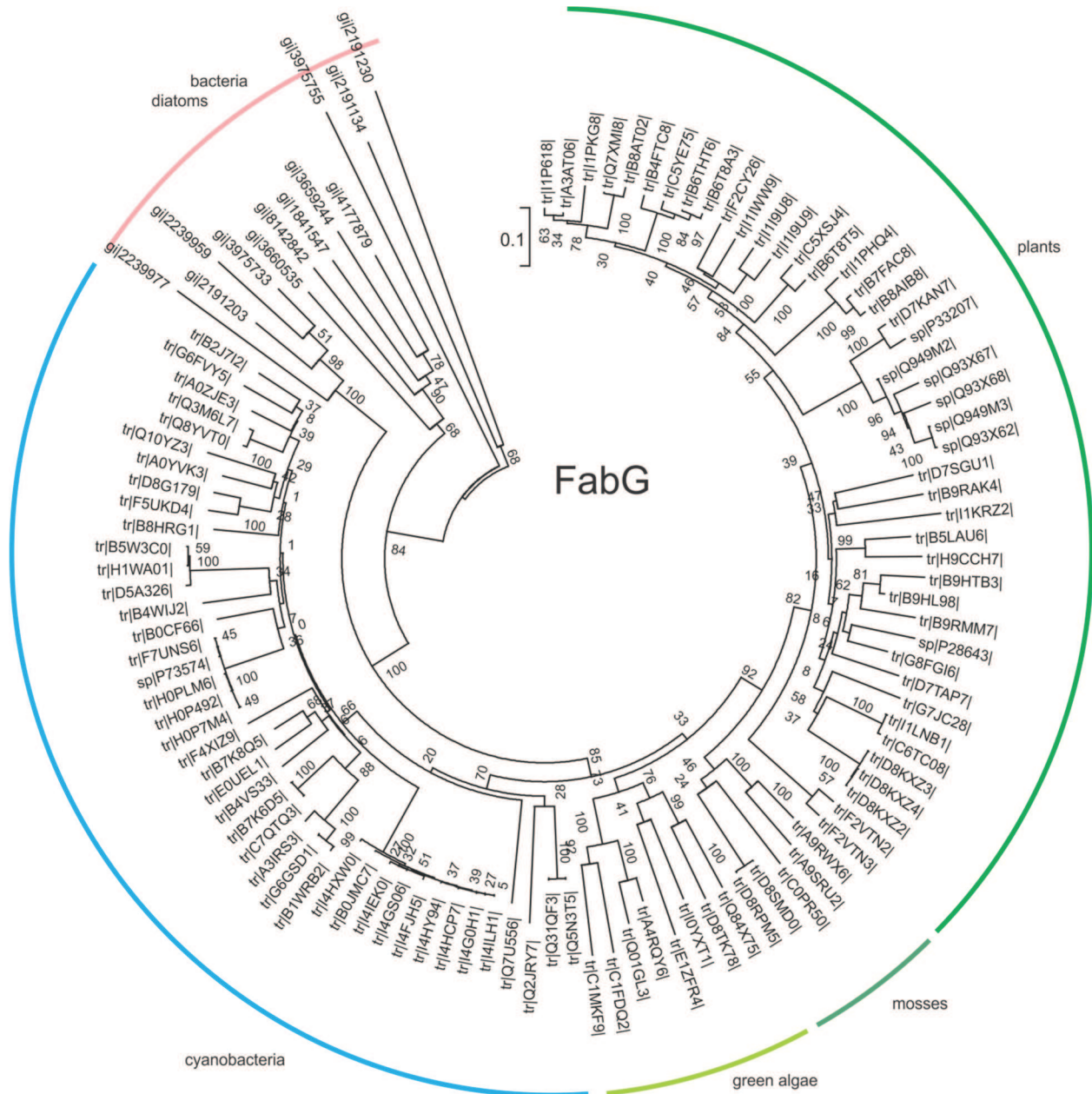


Figure S8 – Phylogeny of ketoacyl ACP reductases (KR, FabG) Neighbour Joining phylogenetic tree, constructed using MEGA 5.2, from 200 plant, algal, cyanobacterial and bacterial FabG sequences.

Figure S9– Phylogeny of acyl-ACP dehydratase (DH, FabZ)

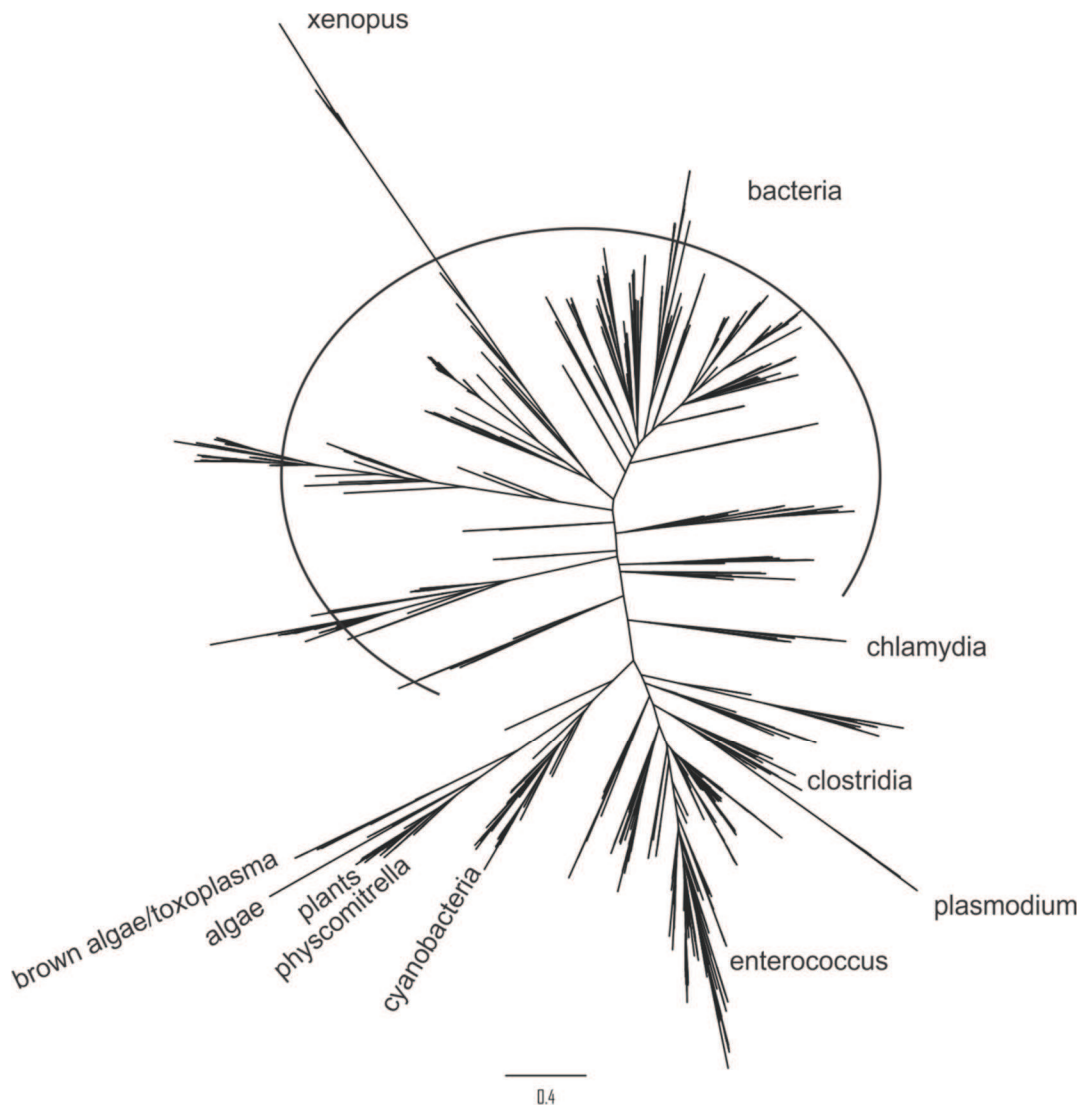


Figure S9 – Phylogeny of dehydratases (DH, FabZ). Sequences were taken together from psi-blasting *C. reinhardtii*'s FabZ and psi-blasting *A. variabilis* FabZ against the entire NCBI genome database and 2000 sequences were analyzed for duplicates (~70%), taxon names shortened using Mesquite, aligned using MUSCLE, a phylogenetic tree built with FastTree and visualized using Figtree.

Figure S10– Phylogeny of acyl-ACP dehydratase (DH, FabZ)

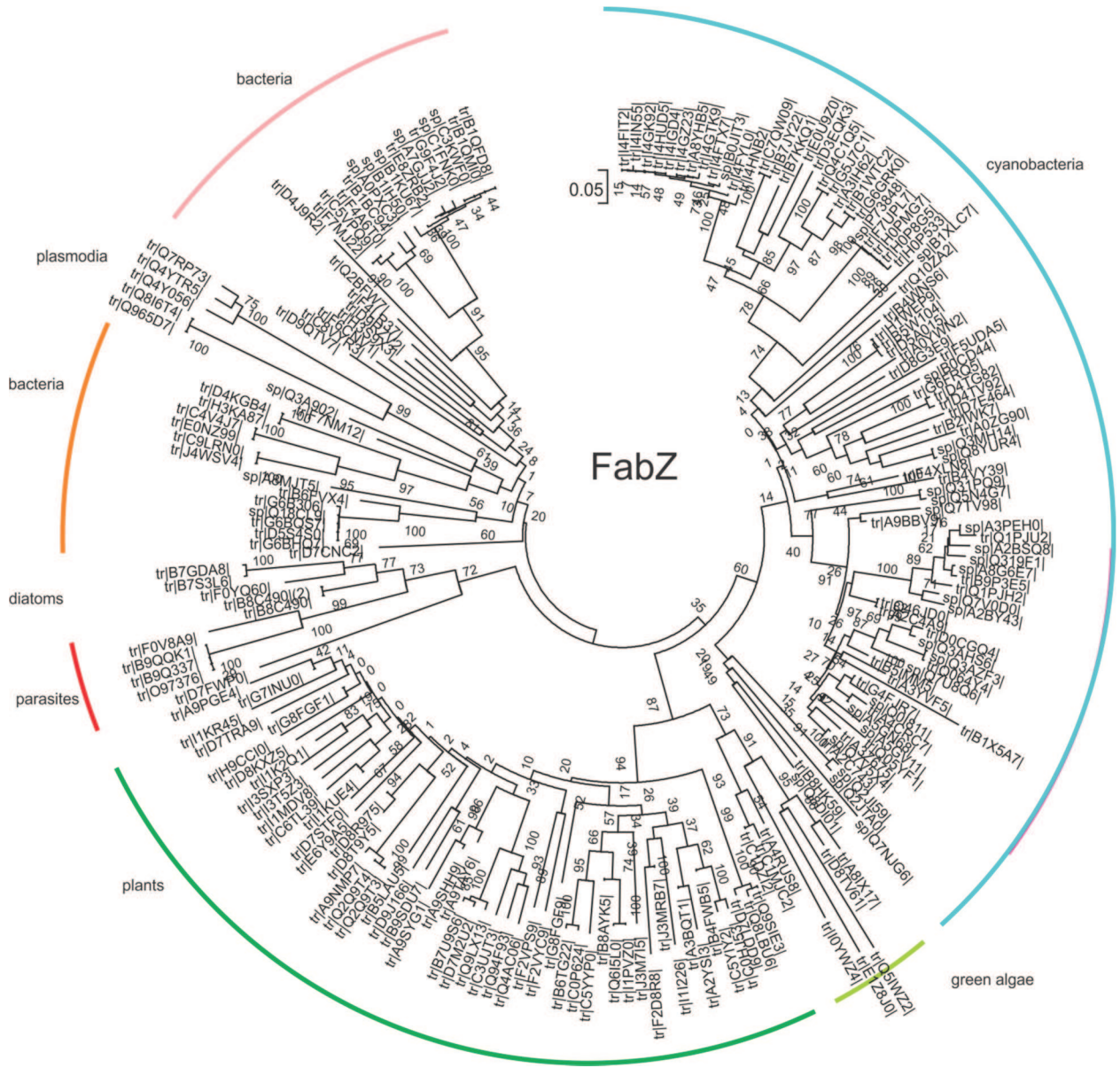


Figure S10 – Phylogeny of dehydratases (DH, FabZ). Neighbor Joining phylogenetic tree, constructed using MEGA 5.2, from 200 plant, algal, cyanobacterial and bacterial FabZ sequences.

Figure S11– Phylogeny of acyl-ACP dehydratase (DH, FabA)

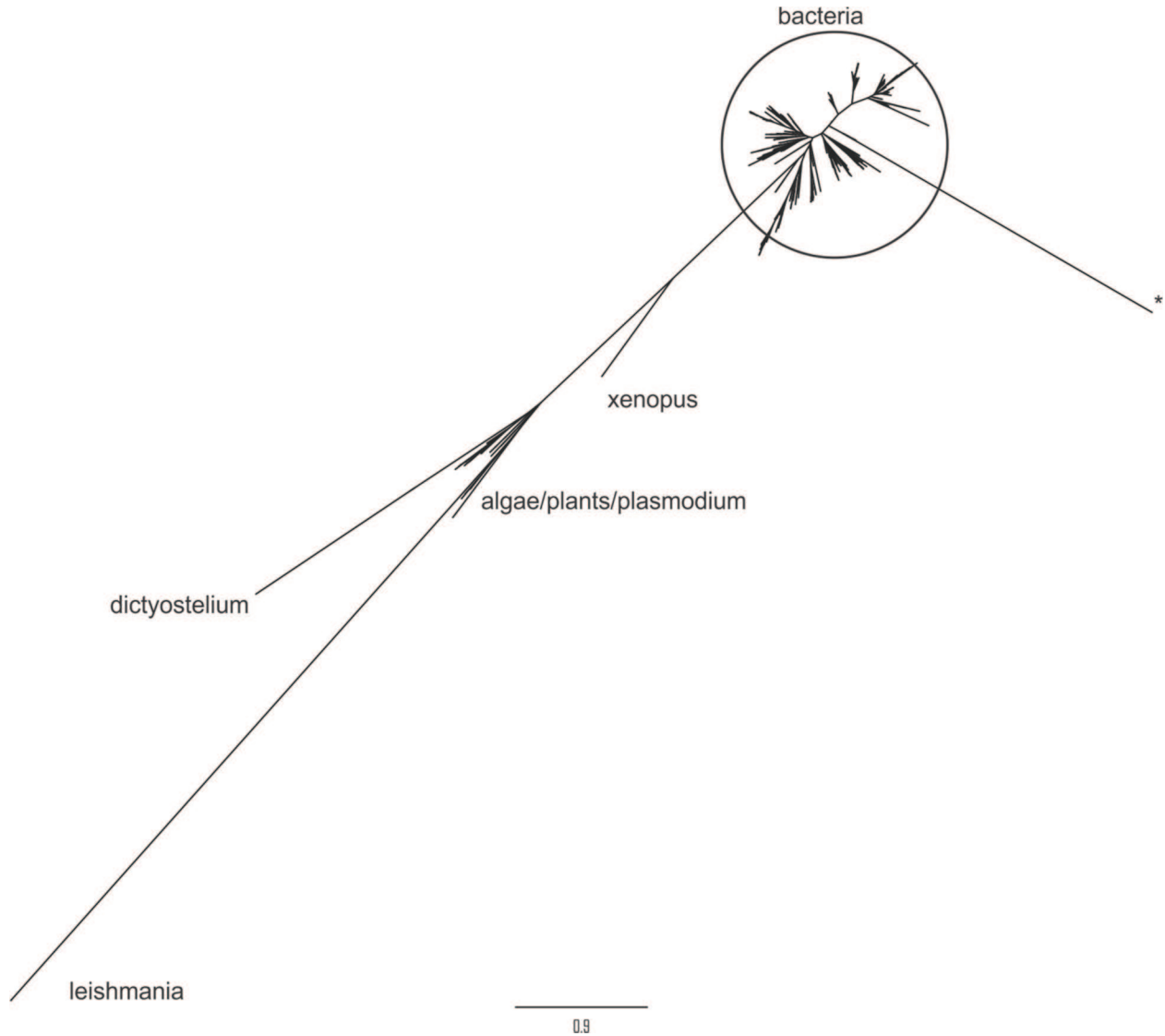


Figure S11 – Phylogeny of acyl-ACP dehydratase FabA. Sequences were taken together from psi-blasting *E. coli*'s FabA against all eukaryotes and, separately, all prokaryotes in the entire NCBI genome database and 2000 sequences were analyzed for duplicates (~5%), taxon names shortened using Mesquite, aligned using MUSCLE, a phylogenetic tree built with FastTree and visualized using Figtree. *) not an acyl-ACP dehydratase but γ -aminobutyric acid type B receptor subunit 2-like protein from *Nasonia vitripennis*.

Figure S12– Phylogeny of enoyl ACP reductase (ER, FabI)

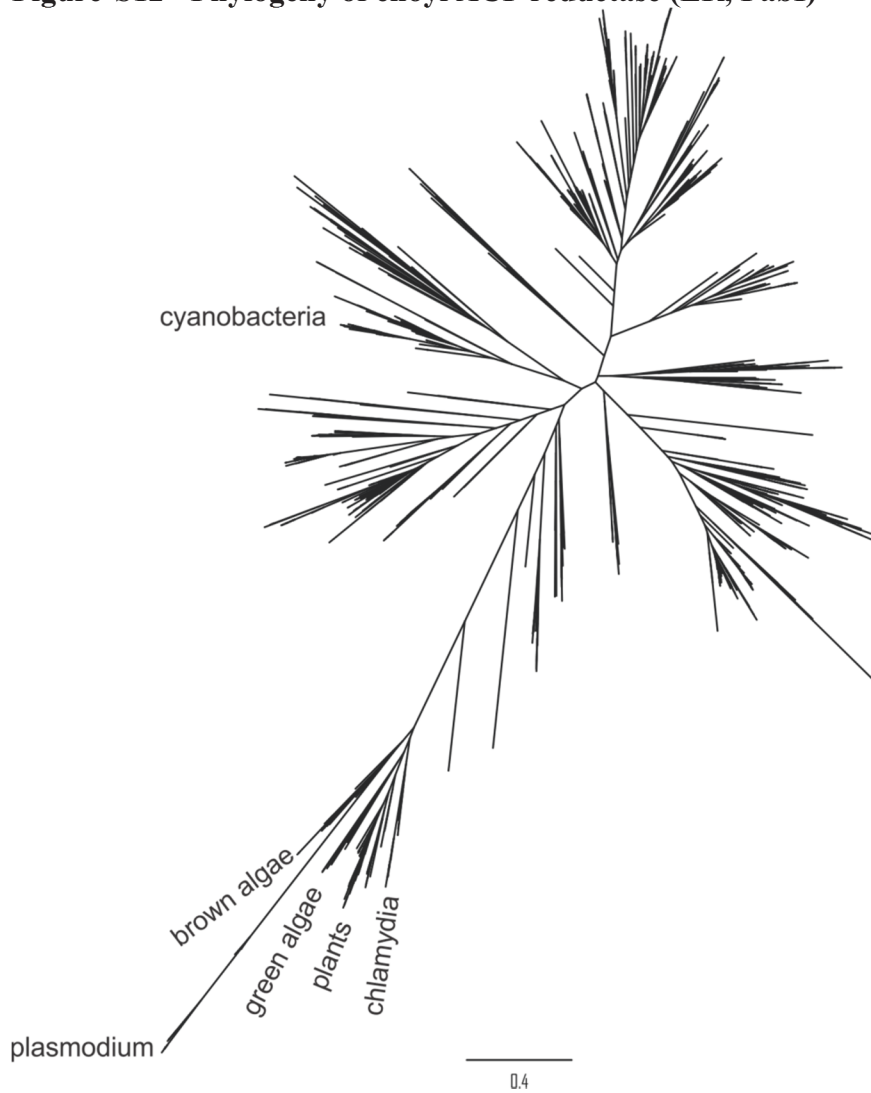


Figure S12 – Phylogeny of enoyl ACP reductases (ER, FabI) Sequences were taken together from psi-blasting *C. reinhardtii*'s ER and psi-blasting *A. variabilis* ER against the entire NCBI genome database and 2000 sequences were analyzed for duplicates (~30%), taxon names shortened using Mesquite, aligned using MUSCLE, a phylogenetic tree built with FastTree and visualized using Figtree.

Figure S13– Phylogeny of enoyl ACP reductase (ER, FabI)

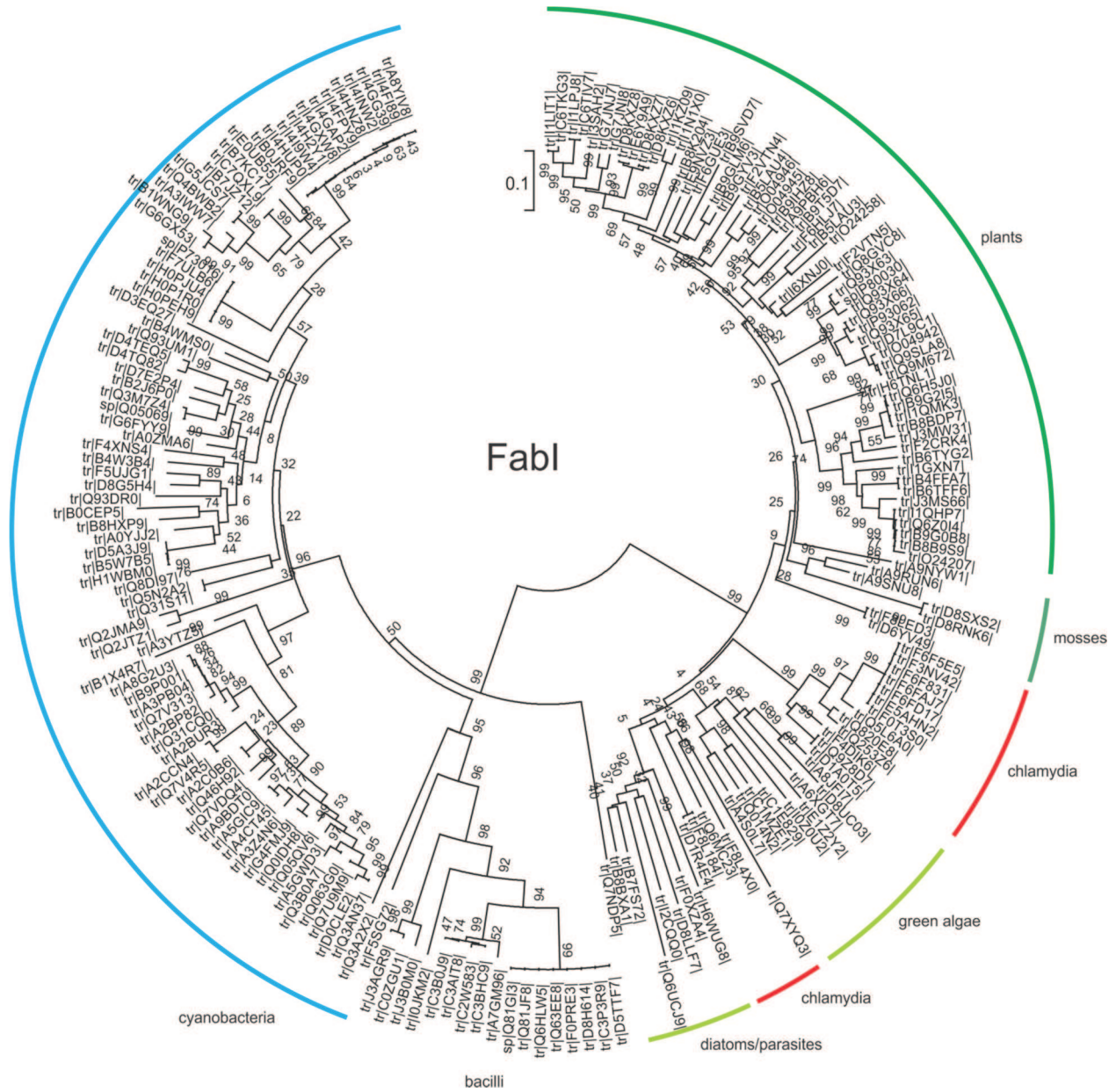


Figure S13 – Phylogeny of enoyl ACP reductases (ER, FabI) Neighbor Joining phylogenetic tree, constructed using MEGA 5.2, from 200 plant, algal, cyanobacterial and bacterial ER sequences.

Figure S14 – Docking of EcACP with various KSs

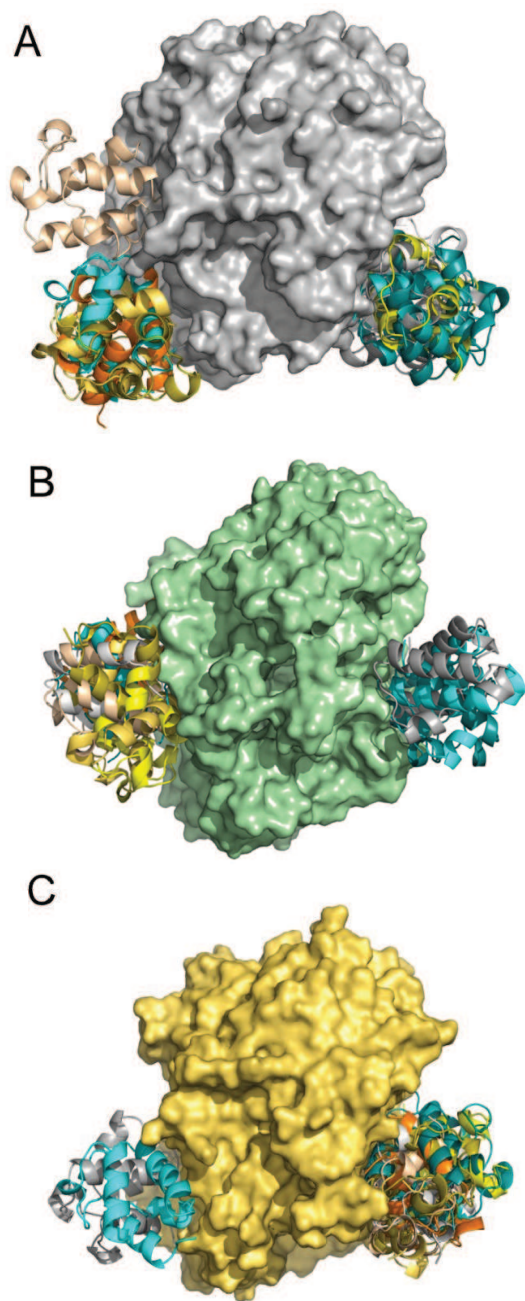


Figure S14 – Ensemble representation of protein-protein docking of EcACP with KSs: the three different KS dimers are shown in surface representation and the top 10 models of docked ACPs in cartoon representation. A) EcKSII (in grey), B) CrKSII (in green), and C) RcKSII (in yellow).

Figure S15 – Docking of extracted EcACP with EcKSII and CrTE

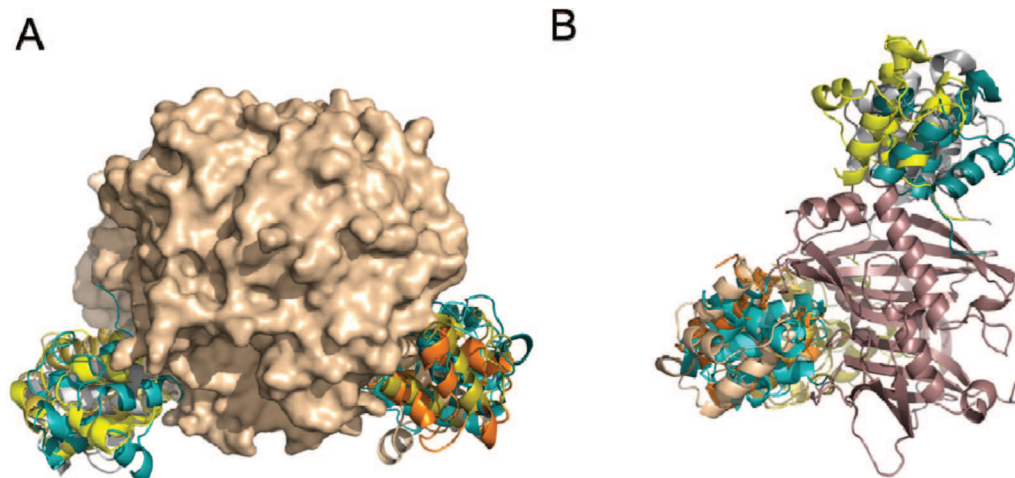


Figure S15 - Ensemble representation of protein-protein docking with extracted EcACP Extracted EcACP docked to A) EcKSII, show in off-white surface representation, and B) CrTE, shown in grey-purple cartoon representation. The top 10 models of EcACP are shown in colored cartoon representation.

Figure S16 – Docking of Cr-cACP with various KSs

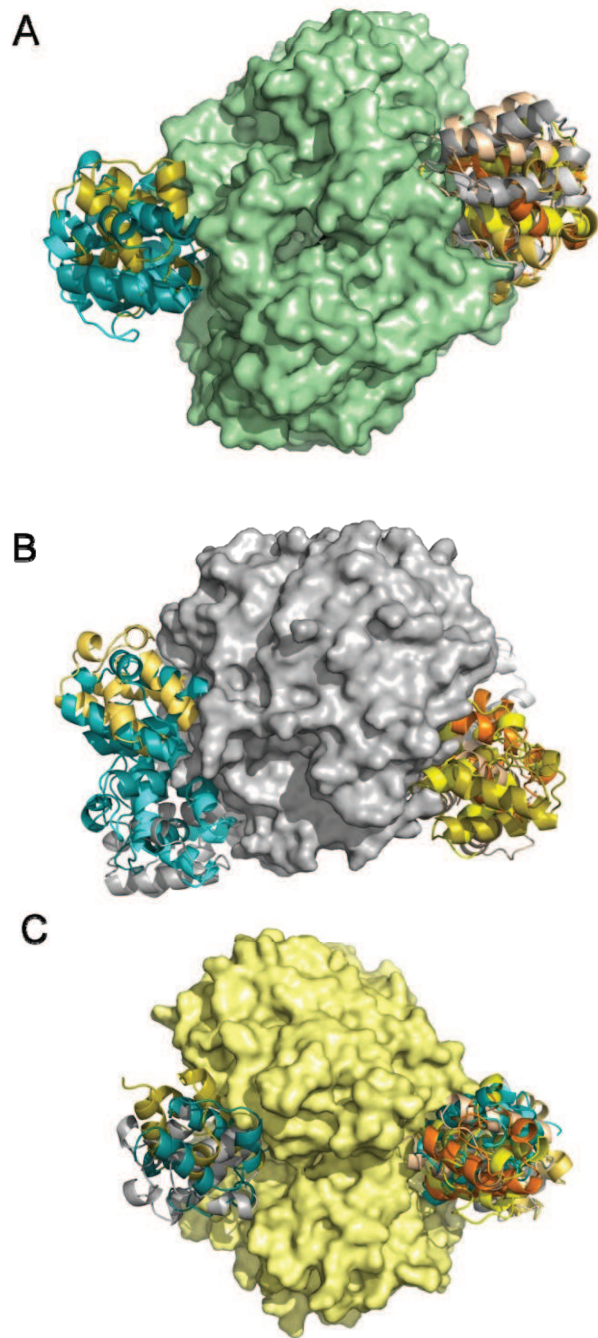


Figure S16 - Ensemble representation of protein-protein docking of Cr-cACP with KSs. The three different KS dimers are shown in surface representation and the top 10 models of docked ACPs in cartoon representation. A) CrKSII (in green), B) EcKSII (in grey) and C) RcKSII (in yellow).

Figure S17 – Docking of RcACP with various KSs

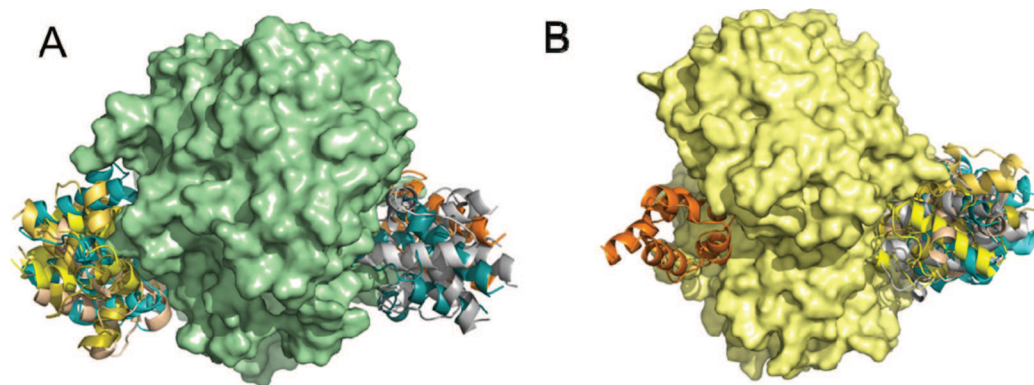


Figure S17- Ensemble representation of protein-protein docking of RcACP with KSs. The two different KS dimers are shown in surface representation and the top 10 models of docked ACPs in cartoon representation. A) CrKSII (in green) and B) RcKSII (in yellow)

Figure S18 – Docking of ACPs with CrTE

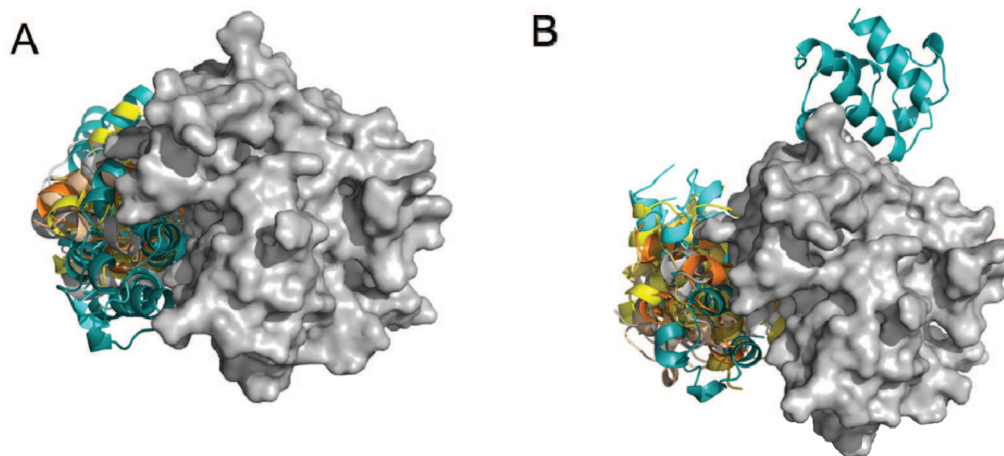


Figure S18 - Ensemble representation of protein-protein docking of EcACP with CrTE. The CrTE is shown in grey surface representation and the top 10 models of docked ACPs in cartoon representation. A) Cr-cACP to CrTE and B) EcACP to CrTE.

Figure S19 – ACP complementation

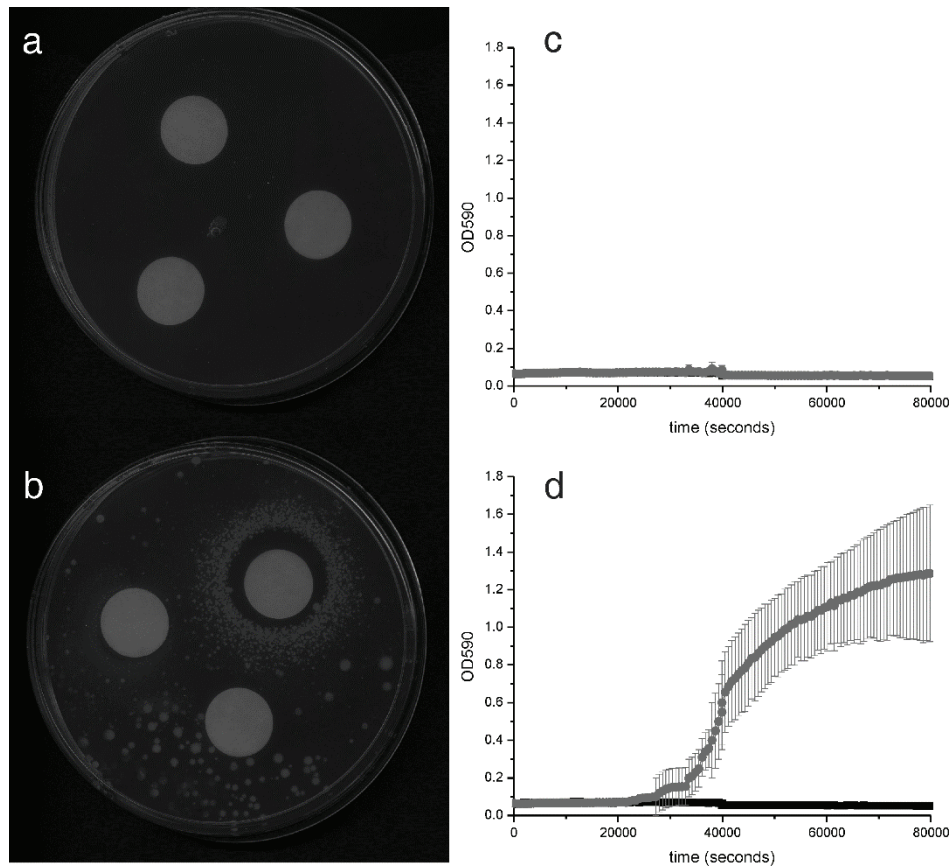


Figure S19 - ACP complementation in vivo. Plasmids encoding Cr-cACP (a) and *Vibrio harveyi* ACP (b) were transformed in chromosomal ACP knock-out *E. coli* strain CY1877, harboring a plasmid with arabinose inducible native EcACP. Dilute cells were plated on LB-agar and 1 pmol IPTG spotted prior to incubation overnight at 37 °C. In parallel, dilute cells expressing Cr-cACP (c) or VhACP (d) were grown in the absence or presence of IPTG. The absorbance at 590 nm was monitored for 2 days while the plate was incubated at room temperature under continuous shaking. Each data point is obtained in triplicate.

Figure S20 – GC/MS profiles of sequenced green microalgae

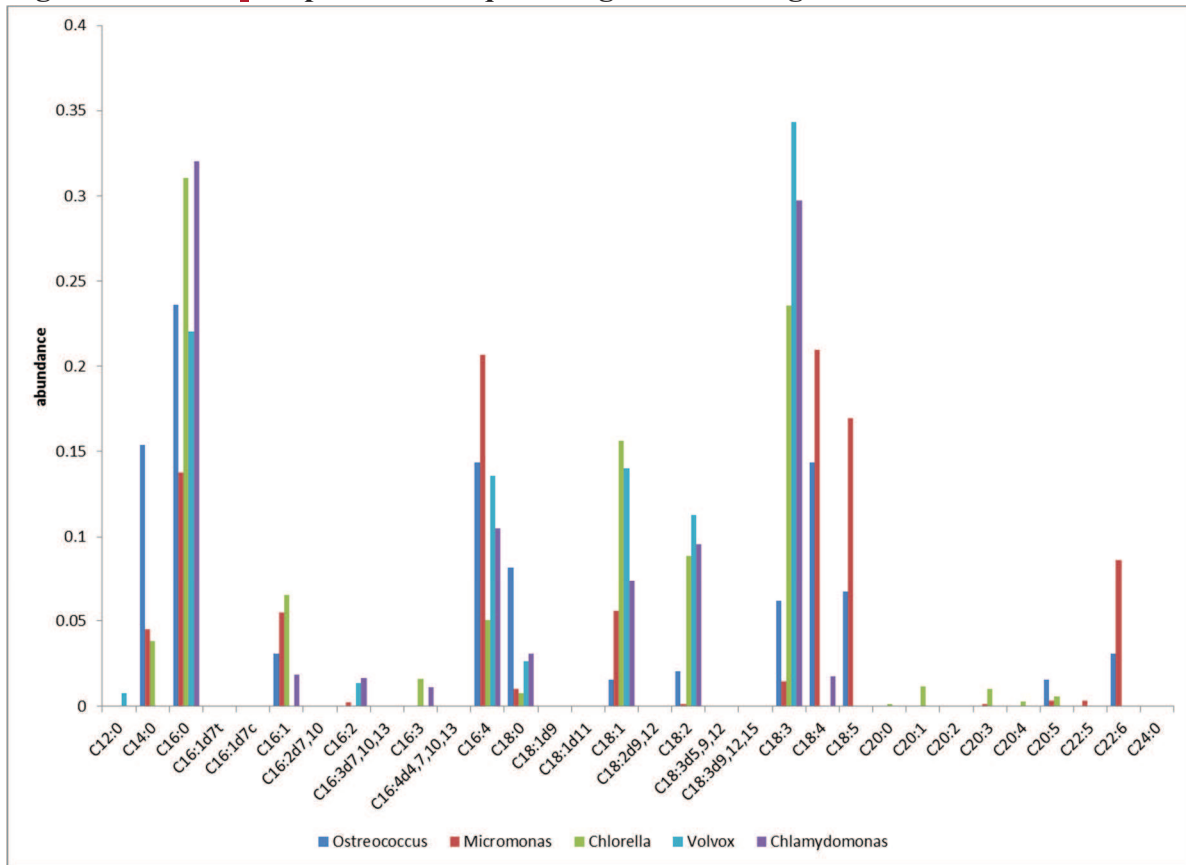


Figure S20 – GC/MS profiles of sequenced green microalgae Fatty acid profiles of sequenced algae: *Ostreococcus lucimarinus* (Ahmann et al. 2011), *Micromonas pusilla* (Dunstan et al. 1992), *Chlorella vulgaris* (Gouveia and Oliveira 2009), *Volvox carteri* (Moseley and Thompson 1980), and *Chlamydomonas reinhardtii* (James et al. 2011).

References

- Ahmann K, Heilmann M, Feussner I (2011) Identification of a Δ^4 -desaturase from the microalga *Ostreococcus lucimarinus*. *European Journal of Lipid Science and Technology* 113 (7):832-840
- Benkert P, Tosatto SC, Schomburg D (2008) QMEAN: A comprehensive scoring function for model quality assessment. *Proteins: Structure, Function, and Bioinformatics* 71 (1):261-277
- Brondz I, Olsen I, Haapasalo M, Van Winkelhoff AJ (1991) Multivariate analyses of fatty acid data from whole-cell methanolysates of *Prevotella*, *Bacteroides* and *Porphyromonas* spp. *Journal of General Microbiology* 137 (6):1445-1452
- Byers DM, Gong H (2007) Acyl carrier protein: Structure-function relationships in a conserved multifunctional protein family. *Biochem Cell Biol* 85 (6):649-662
- Cantu DC, Chen Y, Reilly PJ (2010) Thioesterases: a new perspective based on their primary and tertiary structures. *Protein Sci* 19 (7):1281-1295
- Cantu DC, Forrester MJ, Charov K, Reilly PJ (2012) Acyl carrier protein structural classification and normal mode analysis. *Protein Sci* 21 (5):655-666
- Dunstan GA, Volkman JK, Jeffrey SW, Barrett SM (1992) Biochemical-composition of microalgae from the green algal classes chlorophyceae and prasinophyceae. 2. lipid classes and fatty acids. *Journal of Experimental Marine Biology and Ecology* 161 (1):115-134. doi:10.1016/0022-0981(92)90193-e
- Edgar RC (2004) MUSCLE: Multiple sequence alignment with high accuracy and high throughput. *Nucleic Acids Res* 32 (5):1792-1797
- Edlund A, Nichols PD, Roffey R, White DC (1985) Extractable and lipopolysaccharide fatty acid and hydroxy acid profiles from *Desulfovibrio* species. *Journal of Lipid Research* 26 (8):982-988
- Ghebretinsae AG, Graham SA, Camilo GR, Barber JC (2008) Natural infraspecific variation in fatty acid composition of *Cuphea* (Lythraceae) seed oils. *Industrial Crops and Products* 27 (3):279-287
- Gouet P, Courcelle E, Stuart DI, Métoz F (1999) ESPript: Analysis of multiple sequence alignments in PostScript. *Bioinformatics* 15 (4):305-308
- Gouveia L, Oliveira AC (2009) Microalgae as a raw material for biofuels production. *Journal of Industrial Microbiology and Biotechnology* 36 (2):269-274
- Grimsley NH, Grimsley JM, Hartmann E (1981) Fatty acid composition of mutants of the moss *Physcomitrella patens*. *Phytochemistry* 20 (7):1519-1524
- Guerzoni ME, Lanciotti R, Cocconcelli PS (2001) Alteration in cellular fatty acid composition as a response to salt, acid, oxidative and thermal stresses in *Lactobacillus helveticus*. *Microbiology* 147 (8):2255-2264
- James GO, Hocart CH, Hillier W, Chen H, Kordbacheh F, Price GD, Djordjevic MA (2011) Fatty acid profiling of *Chlamydomonas reinhardtii* under nitrogen deprivation. *Bioresource Technology* 102 (3):3343-3351
- Jing F, Cantu DC, Tvaruzkova J, Chipman JP, Nikolau BJ, Yandea-Nelson MD, Reilly PJ (2011) Phylogenetic and experimental characterization of an acyl-ACP thioesterase family reveals significant diversity in enzymatic specificity and activity. *BMC Biochem* 12 (1)
- Mayberry WR (1980) Hydroxy fatty acids in *Bacteroides* species: D-(--)-3-hydroxy-15-methylhexadecanoate and its homologs. *Journal of Bacteriology* 143 (2):582-587
- Moseley KR, Thompson GA (1980) Lipid composition and metabolism of *Volvox carteri* *Plant Physiology* 65 (2):260-265. doi:10.1104/pp.65.2.260
- Moss CW, Lewis VJ (1967) Characterization of clostridia by gas chromatography. I. Differentiation of species by cellular fatty acids. *Applied Microbiology* 15 (2):390-397
- Notredame C, Higgins DG, Heringa J (2000) T-coffee: A novel method for fast and accurate multiple sequence alignment. *J Mol Biol* 302 (1):205-217
- Siristova L, Melzoch K, Rezanka T (2009) Fatty acids, unusual glycopospholipids and DNA analyses of thermophilic bacteria isolated from hot springs. *Extremophiles* 13 (1):101-109